Operation and performance analysis of direct hollow fiber nanofiltration
A pilot study at IJsselmeer

Ophorst, Marleen; Grooth, Joris de; Heijman, Sebastiaan G.J.; Vaudevire, Elisabeth M.H.; Jafari, Morez

Important note
To cite this publication, please use the final published version (if applicable).
Please check the document version above.

Operation and performance analysis of direct hollow fiber nanofiltration: A pilot study at IJsselmeer

Marleen Ophorst [a,b,*], Joris de Grooth [c], Sebastiaan G.J. Heijman [d], Elisabeth M.H. Vaudevire [b], Morez Jafari [e,b]

[a] *Nazava Water Filters Ltd, Nairobi PRP6+R7V, Kenya*
[b] *PWNT, Nieuwe Hemweg 2, Amsterdam 1013 BG, Netherland*
[c] *NX Filtrations BV, Josink Esweg 44, Enschede 7545 PN, Netherland*
[d] *Delft University of Technology, Civil Engineering Department, Stevinweg 1, Delft 2628 CN, Netherland*
[e] *Oasen, Nieuwe Gouwe O.Z 3, Gouda 2801 SB, Netherland*

A B S T R A C T

This study investigated the performance of direct hollow fiber nanofiltration (dNF40) membranes from NX Filtration BV on a pilot scale for the treatment of pre-treated IJsselmeer water from Waterwinstation Prinses Juliana (WPJ) in Andijk, as well as the direct treatment of raw IJsselmeer water. The objective was to evaluate the long-term fouling potential and the retention of ions and natural organic matter (NOM) using both WPJ pre-treated IJsselmeer water and raw IJsselmeer water. Additionally, the rejection of organic micropollutants (OMPs) under artificially elevated conditions, referred to as 'spiked solution', using WPJ pre-treated IJsselmeer water was investigated.

Limited to no fouling was observed on the dNF40 membrane during stable operation when treating both WPJ pre-treated IJsselmeer water and raw IJsselmeer water, even under changing process conditions. NOM removal consistently exceeded 90% regardless of process conditions or water type. The retention of per- and poly-fluoroalkyl substances (PFAS) was above 80%, with even higher retention observed for higher molecular weight values. Low molecular weight pharmaceuticals, all below the molecular weight cut-off (MWCO) of the dNF40 membrane (400 Da), exhibited approximately 30% retention. The dNF40 membrane showed better retention of negatively charged pharmaceuticals in the spiked solution compared to positively charged and neutral pharmaceuticals.

A total cost of ownership (TCO) analysis unveiled that operational expenditures (OPEX) were three times higher than capital expenditures (CAPEX) for a 5-stage full-scale dNF40 system. Among the components, membrane replacement costs constituted the majority of OPEX (68%), followed by energy costs (31%) and chemical costs (<1%). Overall, the study showcased the suitability of the dNF40 membranes for treating IJsselmeer water, achieving effective removal of NOM and PFAS.

1. Introduction

The water supply company PWN provides an annual supply of 112 billion liters of high-quality drinking water to 804.160 households, businesses, and institutions in the province of North Holland. Their primary water source is the IJsselmeer, a surface water lake. In Andijk, the water undergoes pre-treatment at Waterwinstation Prinses Juliana (WPJ) using conventional methods, including lake aeration, drum screens, coagulation, sedimentation, rapid sand filtration and granular activated carbon filtration. Following pre-treatment, the water is transported to a post-treatment facility in Heemskerk, where ultrafiltration and reverse osmosis (UF-RO) processes yield high-quality permeate. This UF-RO permeate is further conveyed to pompstation (PS) Bergen and Mensink, where it is blended with dune water to produce drinking water with reduced hardness.

UF-RO technology provides the advantage of delivering a biologically stable and high-quality permeate. Nevertheless, the substantial energy consumption and the considerable costs associated with anti-

* Corresponding author.
  E-mail address: marleen.ophorst@gmail.com (M. Ophorst).

scalant in RO operations pose challenges for PWN. Additionally, the permeate from UF-RO necessitates post-conditioning with caustic soda and CO2, owing to low bicarbonate values, before its transportation from Heemskerk to PS Bergen via concrete pipelines. Consequently, PWN is assessing alternative processes and/or membrane types to enhance the UF-RO process.

Recently, drinking water companies have become increasingly vigilant regarding the presence of organic micropollutants (OMPs) and other emerging contaminants. OMPs encompass a diverse array of chemicals found in household products, cosmetics, pesticides, and per- and polyfluoroalkyl substances (PFAS) [1]. Of particular concern in the drinking water industry are PFAS compounds, as they are ubiquitous in numerous consumer products [2]. Their harmfulness resides in both frequent exposure and their capacity to accumulate within human organisms over extended periods [3]. These compounds have been associated with adverse health outcomes such as low infant birth weights, immune system effects, cancer, and thyroid hormone dysfunction [3]. Consequently, regulatory standards for OMP concentrations in drinking water are becoming increasingly stringent.

One of the alternative technologies to UF/RO is nanofiltration (NF) membranes. NF membranes offer distinct separation properties coupled with reduced operating pressures compared to conventional RO membranes [4]. Traditional NF membranes are commonly utilized for applications such as hardness reduction, owing to their ability to retain multivalent ions more effectively than monovalent ions [5]. Additionally, NF membranes have the potential to achieve substantial retention of small (OMPs) [5]. Furthermore, their larger pore size compared to RO membranes leads to reduced bicarbonate retention and consequent reduction in post-conditioning costs.

Several NF membrane configurations are available, including spiral wound membranes, hollow fiber membranes and tubular membranes. Spiral wound membranes are recognized for their high packing density and low module cost [5]. However, they lack hydraulic cleaning capability, necessitating extensive pre-treatment to mitigate fouling [5]. Tubular membranes, on the other hand, allow for hydraulic cleaning and require less pre-treatment [6], albeit at the expensive of lower packing density and higher module cost [6]. In contract, hollow fiber membranes combine the advantages of both spiral wound and tubular membranes [4]. They offer a low fouling potential attributed to effective hydraulic cleaning possibilities [5], making them suitable for filtering fouling-prone feed waters, such as raw surface water.

Among the commercially available hollow fiber NF membranes are the Layer-by-Layer (LbL) hollow fiber NF membranes produced by NX Filtration (NXF). The LbL method represents a versatile technology for the preparation of hollow fiber NF membranes. This method involves the alternating deposition of polyanions and polycations on a charged surface to create polyelectrolyte multilayers (PEMs) [7]. These PEMs form an ultrathin separation layer in the nanometer range, resulting in a chemically and physical stable membrane with versatile retention properties [7]. While most academic research on LbL hollow fiber NF membranes has been conducted using bench-scale membranes with synthetic water [8,9,10], the commercial availability of NXF LbL hollow fiber NF membranes presents an opportunity for practical application and further exploration in real-world scenarios.

This research focuses on a pilot-scale study operating at approximately 1 m³ per hour, utilizing hollow fiber NF membranes for the treatment of WPJ pre-treated IJsselmeer water, as well as the direct treatment of raw IJsselmeer water. The primary objective of this study was to evaluate the long-term fouling potential and the retention of ions and natural organic matter (NOM) using both WPJ pre-treated IJsselmeer water and raw IJsselmeer water, along with the retention of OMPs under artificially elevated conditions ('spiked solution') using WPJ pre-treated IJsselmeer water. The experiments were designed to assess the impacts of membrane process conditions and the background water matrix on the fouling potential and the retention of ions, NOM and OMPs.

2. Materials and methods

2.1. Pilot-scale membrane system

A pilot-scale membrane system featuring a single hollow fiber membrane with a length of 1.4 m, was employed to assess various membrane performance parameters. These parameters included permeability, transmembrane pressure (TMP), normalized pressure drop (NPD), as well as the retention for ions, NOM and OMPs such as PFAS and pharmaceutical compounds. The specific LbL hollow fiber NF membrane model utilized in this study was the dNF40 membrane module manufactured by NX Filtration BV, located in Enschede, NL (Fig. 1). Notably, the dNF40 membrane is characterized by a negative surface charge and possesses a molecular weight cut-off (MWCO) of 400 Da. Comprehensive specifications and operational limits of the dNF40 membrane, as provided by NX Filtration BV, are listed in Table 1.

The study employed two distinct feed solutions, namely WPJ pre-treated IJsselmeer water and raw IJsselmeer water. The WPJ pre-treated IJsselmeer water had undergone a comprehensive pretreatment regimen, including drum screens, coagulation, sedimentation, rapid sand filtration and granular activated carbon filtration. Table 2 provides a detailed breakdown of the water composition for both WPJ pre-treated IJsselmeer water and raw IJsselmeer water. The difference in water quality between pre-treated and raw IJsselmeer water can be attributed to several factors. Specifically, the introduction of ferric chloride (FeCl3) during the coagulation process elevates the chloride concentration, while activated carbon reduces the concentration of NOM. Additionally, HCO3– ions can form insoluble compounds with FeCl3 during coagulation, leading to their partial removal during the sedimentation process.

The pilot system comprised a 150 μm cartridge filter preceding the hollow fiber NF membrane. Operating in a single-stage feed and bleed mode, the hollow fiber NF membrane module was equipped with a feed pump to regulate a prescribed flux and a recirculation pump to control a designated crossflow velocity.

Two distinct experiments were conducted using the pilot system equipped with a single dNF40 module. The first experiment aimed to assess membrane performance parameters, including permeability, TMP and NPD, as well as the retention of ions and NOM. These evaluations were performed under varying operating conditions such as recovery, flux and crossflow velocity. Both WPJ pre-treated IJsselmeer water and raw IJsselmeer water were utilized for this experiment. Notably, the pilot operated in a feedand bleed system configuration during this experiment, wherein the permeate and concentrate were discharged into the sewerage. For simplicity, this experiment will be referred to as

Fig. 1. Dnf 40 membrane module (nx filtration bv, Enschede, NL).

Table 1
Dnf40 membrane specifications and their operational limits.

Parameters	Values
Membrane parameters	
Module length [mm]	1428
External diameter [mm]	200
Module Material (housing-membrane)	PVC-Modified PES
Membrane area [m²]	43
Membrane MWCO	400
Membrane charge	Negative at pH 7
Membrane rejection (MgSO₄) [%]	91
Fiber inner diameter [mm]	0.7
Membrane operational limits	
Max temperature [°C]	40
Operating pH	2——12
Cleaning pH	1——13
Crossflow velocity [m/s]	– 2
Max TMP [bar]	6
Max backwash pressure [bar]	6
Max active chlorine concentration [ppm]	500 at pH > 10

Table 2
Water composition of WPJ pre-treated IJsselmeer water and raw IJsselmeer water.

Parameter	Unit	WPJ pre-treated IJsselmeer water	Raw IJsselmeer water
Ca^{2+}	mg/L	63.8 ± 3.76	65.9 ± 2.21
Mg^{2+}	mg/L	11.5 ± 0.21	11.9 ± 0.51
SO_4^{2-}	mg/L	61.9 ± 2.13	57.7 ± 2.20
Na^+	mg/L	Not measured	50.8 ± 3.64
Cl^-	mg/L	138.1 ± 1.55	91.0 ± 5.04
HCO_3^-	mg/L	149.2 ± 7.48	171.6 ± 2.11
NO_3^-	mg/L	10.4 ± 0.27	10.1 ± 0.48
TOC	mg/L	3.5 ± 0.28	6.2 ± 0.24

Table 3
Summary of the feed water, general pilot settings, membrane performance, and sampled compounds of the feed and bleed experiment and the full recirculation experiment.

	Feed and bleed experiment	Spiked experiment
Aim	Membrane performance parameters Ion retention and NOM removal	OMP retention at elevated concentrations
Feed solution	WPJ pre-treated IJsselmeer water Raw IJsselmeer water	Spiked WPJ pre-treated IJsselmeer water
General pilot operation	Feed and bleed operation Time duration: 1 week Backwash frequency: every 2 h	Full recirculation operation Time duration: 2 h No backwash frequency
Pilot settings	Top-bottom flow direction Air scouring + BW (every 1 filtration cycle) Chemical cleaning between each round No anti-scalant dose	Top-bottom flow direction Chemical cleaning after experiment No anti-scalant dose
Process conditions	See Table 4	See Table 4
Membrane performance	permeability, TMP, NPD	N.A.
Retention	Ions and NOM	OMP under elevated conditions

the"feed and bleed experiment". The second experiment focused on evaluating the retention of OMPs under artificially elevated concentrations, utilizing only WPJ pre-treated IJsselmeer water. During this experiment, the pilot operated in full recirculation mode, with the permeate and concentrate being fed back into the feed vessel. This experiment will be referred to as the "spiked experiment". Table 3 provides a concise overview of both experiments.

2.2. Feed and bleed experiment

A series of experiments were conducted to investigate the long-term fouling potential and retention of ions and NOM by the dNF40 membrane when subjected to WPJ pre-treated IJsselmeer water and raw IJsselmeer water. Throughout these experiments, the pilot system was operated under varying process conditions, with alterations made to recovery, flux, or crossflow velocity (designated as rounds A − J, as detailed in Table 4). The chosen process conditions aimed to explore the operational extremes of the pilot system while adhering to the system limits specified by NXF (refer to Table 1). Additionally, these conditions were designed to mitigate fouling potential and minimize water loss. Each experimental round spanned a continuous operation period of 7 days. During filtration, the pilot system operated in a cyclic mode, featuring filtration cycles lasting 120 min, alternated with 60 second hydraulic cleaning cycles. The hydraulic cleaning cycles comprised

backwash and air scour procedures in combination with forward flush. Notably, the flow direction during filtration was from top to bottom, while it was reversed during hydraulic cleaning cycles. This hydraulic cleaning protocol, recommended by NXF, aimed to mitigate fouling formation.

Membrane performance parameters, including permeability, TMP, and NPD, were generated for each experimental round to evaluate the membrane's fouling potential (Equations (1)–(3)). The parameters were normalized to a temperature of 20°C to adjust for temperature variations, ensuring consistency. This normalization process followed empirical Equations (5)–(8). It is worth noting that these formulas do not account for osmotic pressure, which is also temperature-dependent.

Ion and NOM retention were determined by calculating the difference between the concentrations of ions and NOM in the feed and permeate streams (Equation (4)). In this study, NOM was quantified as total organic carbon (TOC). Duplicate samples of ions and TOC were collected after 7 days of pilot operation. Subsequently, ion and TOC concentrations were analyzed at het Waterlaboratorium N.V. (HWL) in Haarlem, the Netherlands. In round F, additional parameters related to NOM, including acids, biopolymers, building blocks, hydrophobic organic compounds, humic substances, neutrals, and particulate organic matter, were analyzed using liquid chromatography – organic carbon detection (LC-OCD).

$$Permeability = \frac{J}{TMP} \tag{1}$$

$$TMP = \frac{P_F + P_C}{2} - P_P + static height correction \tag{2}$$

$$NPD = P_F - P_C - static height correction \tag{3}$$

$$R = \left(1 - \frac{c_P}{c_F}\right) * 100\% \tag{4}$$

$$TMP_{TC} = TMP * 497 * (42.5 + T)^{-1.5} \tag{5}$$

$$NPD_{TC} = NPD * 0.02582 * 10^{\frac{247.8}{T+133}} \tag{6}$$

$$NPD_{flow_{TC}} = |NPD_{TC} - static height correction| \tag{7}$$

Table 4
Timeline process settings and conditions.

Experiment	Start date	Water type	Recovery [%]	Flux [LMH]	Crossflow velocity [m/s]
Round A	07–04–2021	Pre-treated IJsselmeer	70	20	0.2
Round B	14–04–2021		80	20	0.2
Round C	28–04–2021		90	20	0.2
Round D	06–05–2021		90	25	0.2
Round E	02–08–2021		90	20	0.3
Round F	01–11–2021	Raw IJsselmeer	70	20	0.2
Round G	08–11–2021		80	20	0.2
Round H	15–11–2021		90	20	0.2
Round I	22–11–2021		70	25	0.2
Round J	29–11–2021		70	20	0.5
Round K	26–08–2021	Spiked pre-treated IJsselmeer	70	30	0.2

$$Permeability_{TC} = Permeability * \frac{0.02414*10^{\frac{247.8}{T+273-140}}}{0.02414*10^{\frac{247.8}{20+273-140}}} \qquad (8)$$

2.3. Spiked experiment

The OMP retention of the dNF40 membrane was assessed using spiked WPJ pre-treated IJsselmeer water. For this experiment, the pilot operated at 70% recovery, 30 LMH flux, and 0.2 m/s crossflow velocity (designated as round K in Table 4). These process conditions were carefully selected to minimize fouling potential and water loss. During the experiment, the pilot system operated in full recirculation mode, wherein the permeate and concentrate were continuously recycled back to the feed vessel. This operational approach aimed to prevent any potential leakage of harmful OMPs into the environment. It is noteworthy that operating in full recirculation mode resulted in a 1°C temperature increase after 2 h of pilot operation.

The OMP retention experiment was conducted using spiked WPJ pre-treated IJsselmeer water. To encompass a broad spectrum of OMPs, a multi-element solution containing PFAS, negatively charged, neutral, and positively charged pharmaceuticals was introduced into the water. These OMPs in the multi-element solution were representative of those found in the IJsselmeer. The spiked feed solution was prepared by diluting 1 L of the OMP-containing stock solution into the 1000 L feed vessel with WPJ pre-treated IJsselmeer water. The concentrations of the OMPs in the spiked feed solution are detailed in Table 5. Notably, the concentration in the multi-element solution was 100 times higher than that of the OMPs in the pre-treated IJsselmeer water. This ensured that even with maximum removal efficiency, the measured concentration in the permeate remained above the analytical detection limit.

OMP retention was determined by comparing the concentrations of OMPs in the feed and permeate streams using Equation (4). Samples for OMP analysis were collected after 2 h of operation. This duration was

selected to reach a steady-state filtration regime and ensure that PFAS adsorption on the membrane surface reached saturation. PFAS and pharmaceutical concentrations were analyzed at het Waterlaboratorium N.V. (HWL) in Haarlem, the Netherlands.

2.4. Chemical cleaning of the membrane

During the feed and bleed experiment, the pilot operated in cyclic mode, alternating between filtration mode and backwash mode, along with air scour mode combined with a forward flush.

No chemical enhanced backwash was utilized and anti-scalant was not introduced during the experiments.

Chemical cleaning of the membrane was conducted after each change in process condition. This cleaning-in-place (CIP) procedure involved alkaline cleaning (30 ppm NaOH, 130 ppm NaOCl, pH 12, 30 min), followed by a 1-minute rinse with permeate, and subsequently, acid cleaning (3200 ppm citric acid, pH 3, 30 min), followed by another 1-minute rinse with permeate.

2.5. Economic analysis

Following the outcomes of the raw IJsselmeer water studies conducted on the pilot, NX Filtration BV has provided a projection report of a full-scale hollow fiber NF plant utilizing dNF40 membranes for an economic analysis. The production capacity of this full-scale hollow fiber NF plant is comparable with that of the UF-RO plant in Heemskerk (15 M m3/year). The projection report depicts details such as the number of membranes, applied pressure, and chemical requirements for the full-scale dNF40 plant. Comprehensive specifications for the full-

Table 5
PFAS and pharmaceutical compounds in the spike solution, their molecular weights, and the intended concentration.

Category	Compound	MW [g/mol]	Concentration in spike solution [µg/L]
PFAS	PFOS	500	0.1
	PFNA	464	0.02
	PFOA	414	0.1
	PFHxS	400	0.1
Negative pharmaceuticals	Diclofenac	296	2
	Sulfamethoxazole	253	2
Neutral pharmaceuticals	Carbamazepine	236	2
	Gabapentin	171	2
	Benzotriazole	119	2
	Pyrazol	68	2
Positive pharmaceuticals	Sotalol	272	2
	Metoprolol	267	2
	Metformin	129	2
	Melamine	126	2

Table 6
Plant specifications, feed water parameters and membrane performance parameters of the full-scale dNF40 plant.

Variables	Units	Full-scale dNF40 plant
Plant characteristics		
Feed water source	[-]	Raw IJsselmeer water
Years of operation	Years	5
Production capacity	m³/year	15.000.000
Water recovery	%	85
Membrane type	[-]	WRC200-dNF40-IRD
CIP frequency	CIP/year	13
CIP duration	hours/event	1
Number of stages	[-]	5
Number of modules	[-]	1535
Performance parameters		
Average applied pressure	kWh/m³	0.19
Design flux	LMH	22.3
Chemical information		
NaOH (30 %)	ton/year	0.68
NaOCl (12.5 %)	ton/year	1.14
Citric acid (50 %)	ton/year	6.29

scale dNF40 plant are presented in Table 6.

A total cost of ownership (TCO) analysis was conducted according to these specifications. The TCO has been simplified into operational expenditure (OPEX) and capital expenditure (CAPEX). The OPEX comprises the energy cost, chemical cost, and membrane replacement cost [11]. Waste disposal costs and labor cost were neglected from consideration due to the absence of information specific to NF. The CAPEX encompassed the equipment and installation cost [11]. Other potential CAPEX, such as land acquisition, planning, and construction of buildings were neglected as they are highly case-dependent and subjective.

The energy cost, chemical cost, and membrane replacement cost were calculated using Equations (9)–(11) respectively, where P_f represents the average applied pressure (including feed pump, recirculation pumps, and hydraulic cleaning pumps), Q_f stands for the feed flow, $V_{chemical}$ denotes the volume of the chemical, t represents the operation time (set as 5 years, as per Table 6), and N_{module} represents the number of modules. Additional relevant cost factors for the OPEX calculations are outlined in Table 7.

The equipment and installation cost were determined by considering the number of membrane modules and the unit price of each module (Cf_{module}). For auxiliary components such as pipes, pumps and valves, a comparable price to that of the membrane was applied. The calculation of the equipment and installation cost was calculated using Equation (12).

$$\text{\euro}_{energy} = \frac{Cf_e}{\eta} * P_f * Q_f \tag{9}$$

$$\text{\euro}_{chemical} = \sum Cf_c * V_{chemical} \tag{10}$$

$$\text{\euro}_{membrane} = \frac{Cf_{module}}{t} * N_{module} \tag{11}$$

$$\text{\euro}_{equipment\&installation} = 2 * Cf_{module} * N_{module} \tag{12}$$

3. Results and discussion

3.1. Membrane performance parameters: Fouling potential

The membrane performance parameters, including permeability, TMP, and NPD were monitored to assess the long-term fouling potential of the dNF40 membrane. These parameters were normalized to a temperature of 20°C using Equations (5)–(8) to facilitate fair comparisons. Fig. 2 illustrates the trends in (a) permeability, (b) TMP, and (c) NPD observed during filtration rounds A − E when using WPJ pre-treated IJsselmeer water. Fig. 3 depicts the trends in (a) permeability, (b) TMP, and (c) NPD observed during filtration rounds F − J with raw IJsselmeer water. Each vertical line in the figures represents a change in operating conditions as shown in Table 4.

A smaller operational interval was observed during rounds E, I, and J as indicated in both Fig. 2 and Fig. 3. These interruptions were primarily due to emergency shutdowns triggered by various factors. In round E, the shutdown was prompted by the pump operating near its maximum capacity, a consequence of elevated feed water temperature (typical of

summer conditions) and high recovery rates. In round I, the pump neared its maximum capacity owing to lower feed water temperature (typical of winter conditions), reduced recovery rates, and higher flux. In round J, the pilot was inactive during the weekend as it lacked access to the feed water. Following these emergency shutdowns, the pilot was restarted to resume the experimental procedures.

The membrane performance parameters were monitored to assess the long-term fouling potential under constant process conditions (Table 4). Against expectations, limited to no fouling was observed on the dNF40 membrane when the pilot was operated with WPJ pre-treated IJsselmeer water (Fig. 2) and raw IJsselmeer water (Fig. 3). Remarkably, all membrane performance indicators remained stable between each vertical line, contradicting numerous reports in the literature citing decreases in NF membrane permeabilities due to fouling formation [13−17]. For instance, Frank et al. [6] observed a decline in flux attributable to fouling when using bench-scale spiral wound and hollow fiber NF membranes operated with raw surface water from the river Rhine at Arnhem. Compared to spiral wound NF membranes, hollow fiber NF membranes exhibit lower fouling potential due to the absence of a spacer and the possibility of backwash cleaning [6]. One possible explanation for the limited to no fouling observed could be attributed to the regular backwash cleaning every 2 h and the low surface roughness of the membrane. It is known that the hydrophilic and smooth surfaces of PEMs are less prone to fouling [18].

The slight fluctuations in membrane performance observed in specific rounds may be attributed to temperature variations. Although permeability, TMP, and NPD were adjusted to a standard temperature of 20°C to accommodate the alterations in viscosity and density resulting from varying feed water temperatures, it appears that not all factors influencing membrane performance were fully accounted for during normalization. Relying solely on viscosity and density adjustments might not have been comprehensive enough for complete normalization.

The influence of the different compositions of the two water sources, pre-treated IJsselmeer water and raw IJsselmeer water (Table 2), on the fouling potential was assessed by monitoring membrane performance parameters. Despite the higher concentrations of NOM in raw IJsselmeer water compared to WPJ pre-treated IJsselmeer water (6.2 mg/L C and 3.5 mg/L C respectively), fouling formation on the membrane was not observed (Figs. 2 and 3). This finding contradicts with existing literature, as NOM typically serves as a primary fouling constituent in surface water and significantly contributes to fouling on membrane surfaces [19]. The membrane's resistance to fouling formation suggests its suitability for direct application to feed waters prone to fouling, such as raw surface water.

The effect of changing process conditions was systematically evaluated by monitoring the membrane performance parameters. The recovery was incrementally increased from 70% to 80% and 90% in rounds A, B and C with WPJ pre-treated IJsselmeer water and rounds F, G, and H with raw IJsselmeer water (Table 4). An increase in recovery with WPJ pre-treated IJsselmeer water exhibited marginal impact on the permeability (7.0 LMH/bar) (Fig. 2a). Interestingly, in the case of raw IJsselmeer water (Fig. 3a), a slight increase in permeability was observed between rounds F and G (8.5 LMH/bar) compared to round H (9.1 LMH/bar). This unexpected trend may be attributed to factors such as temperature elevation from 6.8 °C in round F and G to 9.6 °C in round H, or other operational parameters. For instance, Emamjomeh et al. [20] demonstrated that elevated water temperatures induce expansion of the membrane material, leading to an enlargement of pores and consequently higher permeability. Further investigation into this phenomenon will be conducted in Chapter 3.3.

The flux was increased from 20 LMH to 25 LMH in rounds C and D with WPJ pre-treated IJsselmeer water and rounds F and I with raw IJsselmeer water (Table 4). An increase in flux resulted in a corresponding increase in TMP, rising from 4.5 bar in round C to 5.5 bar in round D (Fig. 2b). This observation aligns with existing literature,

Table 7
Cost factors for the OPEX calculations.

Cost factor	Symbol	Unit	Value
Power supply efficiency	η	[-]	0.8 [12]
Electricity cost	Cf_e	€/kWh	0.10 [12]
NF membrane module price	Cf_{module}	€/module	2500 [a]
Chemical cleaning cost	Cf_c		
NaOH (30 %)		€/ton	300
NaOCl (12.5 %)		€/ton	240
Citric acid (50 %)		€/ton	1500

[a] Indicative total nanofiltration (NF) module price (inside battery limits).
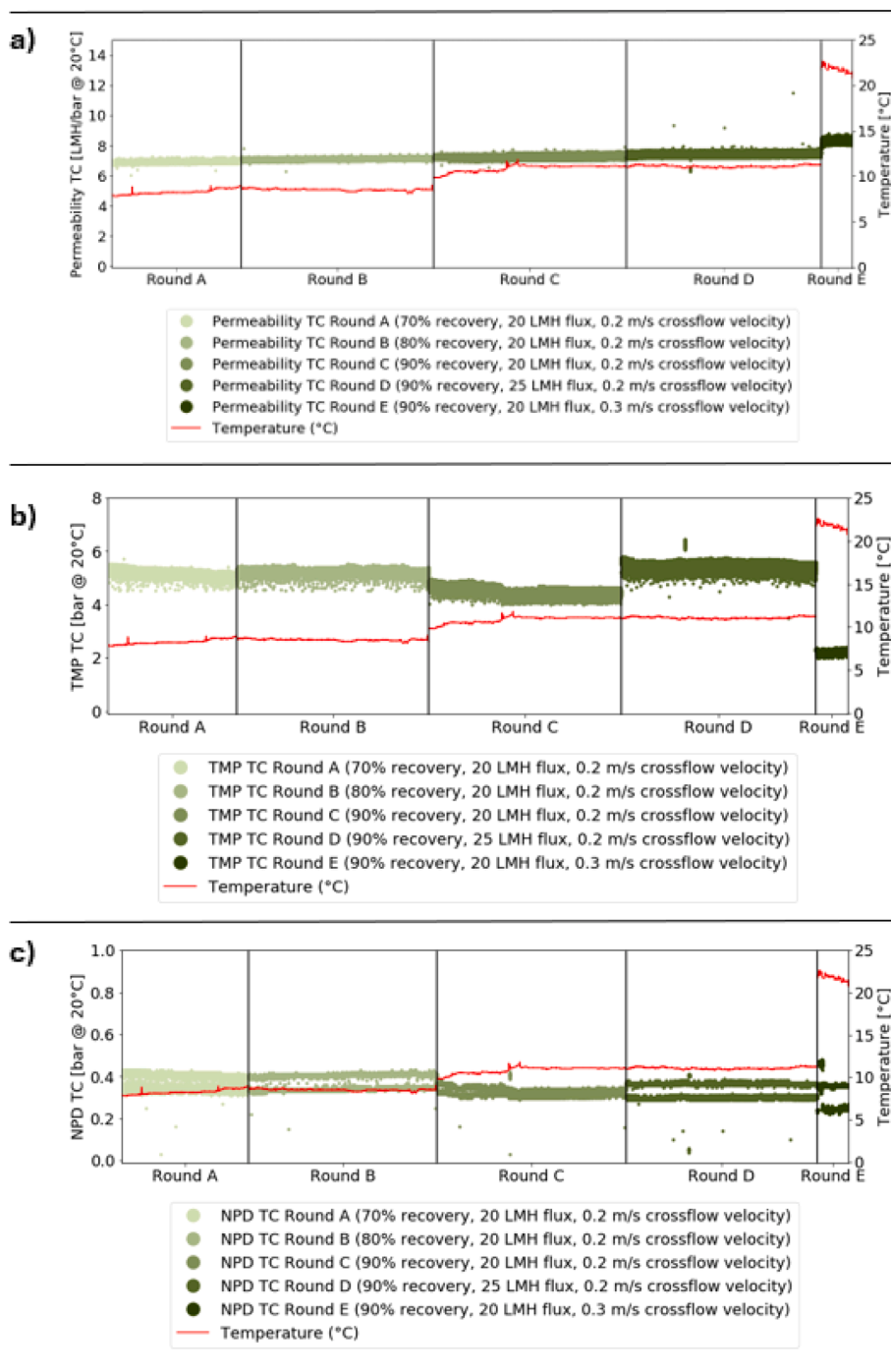
Fig. 2. The a) permeability, b) trans membrane pressure, and c) normalized pressure drop temperature corrected during filtration with **pre-treated IJsselmeer water**. The red line indicates the temperature of the feed water. With each filtration round, denoted by the vertical lines, there was a modification in process conditions, as detailed in Table 4. (For interpretation of the references to colour in this figure legend, the reader is referred to the web version of this article).

suggesting that membrane fouling may occur when the critical flux is surpassed, causing the module to operate beyond the linear relationship between flux and TMP [6]. In the absence of fouling, TMP should rise proportionally with increasing flux [21], hence the higher TMP recorded in round D compared to round C for WPJ pre-treated IJsselmeer water. However, with raw IJsselmeer water, an increase in flux had minimal impact on TMP, with readings of 4.8 bar in round F and 4.6 bar in round I (Fig. 3b). This occurrence could potentially be attributed to the slightly higher temperature in round I (9.0 °C) compared to round F (6.9 °C). Elevated feed water temperatures necessitate lower TMP to sustain the desired flux due to material expansion in the membrane [20].

The crossflow velocity was increased from 0.2 m/s in round C to 0.3 m/s in round E with WPJ pre-treated IJsselmeer water, and from 0.2 m/s in round F to 0.5 m/s in round J with raw IJsselmeer water, (Table 4). It is anticipated that the risk of fouling diminishes as crossflow velocity increases [22]. With raw IJsselmeer water (Fig. 3c), the increased crossflow velocity influenced NPD values by nearly a factor of 2, with 0.83 bar in round F compared to 0.44 bar in round J. Increased crossflow velocities require greater energy input for feed circulation, thereby resulting in higher NPD values. An increase in crossflow velocity with WPJ pre-treated IJsselmeer water (Fig. 2c) showed minimal impact on the NPD, possibly attributed to the high temperature increase.
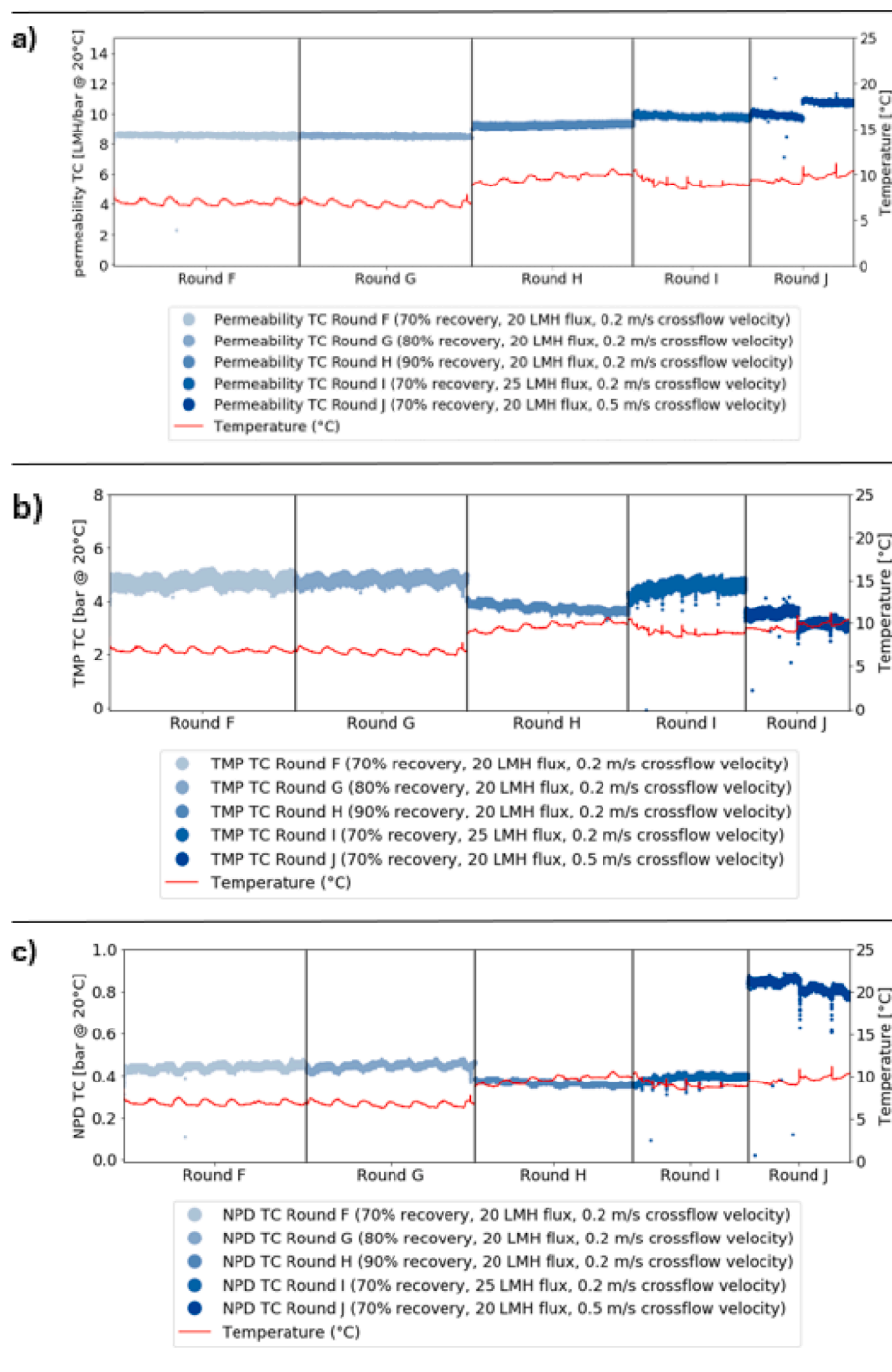
Fig. 3. The a) permeability, b) trans membrane pressure, and c) normalized pressure drop temperature corrected during filtration with **raw IJsselmeer water**. The red line indicates the temperature of the feed water. With each filtration round, denoted by the vertical lines, there was a modification in process conditions, as detailed in Table 4. (For interpretation of the references to colour in this figure legend, the reader is referred to the web version of this article).

3.2. Ion retention WPJ pre-treated and raw IJsselmeer water

The evaluation of ion retention using the dNF40 membrane entailed conducting experiments under various process conditions (refer to Table 4) utilizing both pre-treated and raw IJsselmeer water. Fig. 4 illustrates the ion retention observed during each filtration round using WPJ pre-treated IJsselmeer water, while Fig. 5 presents the ion retention observed during each filtration round using raw IJsselmeer water.

Ions are predominantly retained by size (steric) exclusion and Donnan (charge) exclusion [9]. The membrane's retention mechanism is primarily governed by divalent ions such as SO_4^{2-}, Ca^{2+}, and Mg^{2+} rather than monovalent ions like Na^+, Cl^-, HCO_3^- and NO_3^- (Figs. 4 and 5), owing to their larger hydrated size and charge (Table 8)) [9,23]. The negative terminal layer of the hollow fiber NF membrane exhibits typical Donnan exclusion behavior, resulting in higher retention values for the negative multivalent ion SO_4^{2-} compared to the positive multivalent ions Ca^{2+} and Mg^{2+}. It is noteworthy that Donnan exclusion also contributes to the rejection of positive charged ions like Ca^{2+} and Mg^{2+}, facilitated by the alternating positive and negative layers within the LbL membrane structure. Within a polyanion-polycation multilayer, an excess of polycations can generate surplus positive charge, thereby repelling the cations [24]. However, this repulsion of cations is impeded by the negative
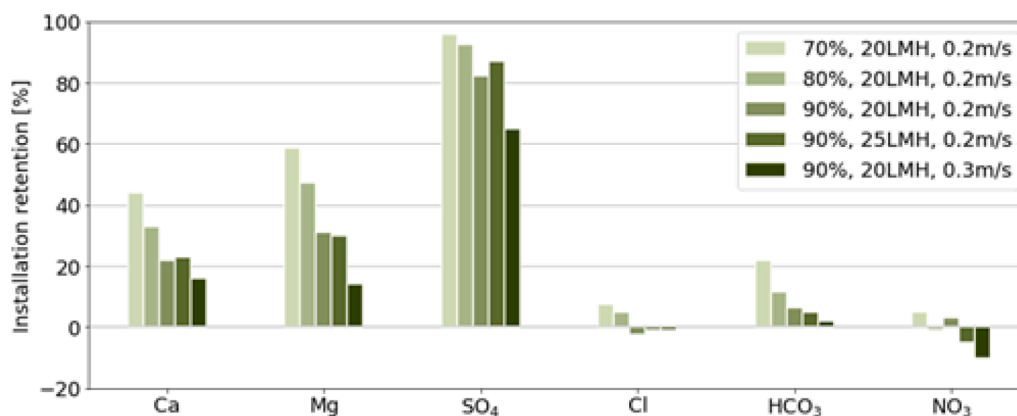
Fig. 4. Ion installation retention based on concentrations measured in feed stream and permeate stream during filtration with **pre-treated IJsselmeer water**. (For interpretation of the references to colour in this figure legend, the reader is referred to the web version of this article).

Fig. 5. Ion installation retention based on concentrations measured in feed stream and permeate stream during filtration with **raw IJsselmeer water**. (For interpretation of the references to colour in this figure legend, the reader is referred to the web version of this article).
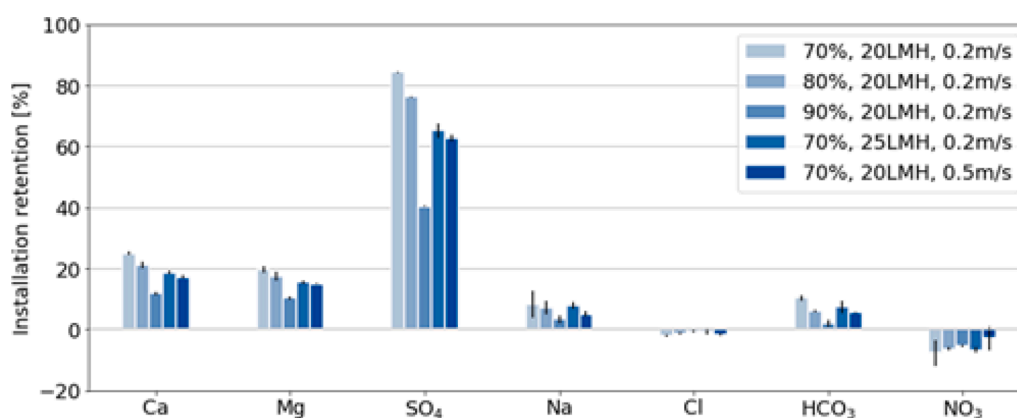
Table 8
Molecular weight (MW), hydrated radius, and ionic radius of the ion compounds [20].

Ion compound	MW [g/mol]	Hydrated radius [mm]	Ionic radius [mm]
Ca^{2+}	40.1	0.412	0.100
Mg^{2+}	24.3	0.428	0.072
SO_4^-	96.1	0.379	0.290
Na^+	23.0	0.358	0.102
Cl^-	35.5	0.332	0.181
HCO_3^-	61.0	0.364	0.156
NO_3^-	62.0	0.335	0.264

terminal layer of the membrane, explaining the lower retention values for Ca^{2+} and Mg^{2+}.

Cheng et al. [9] investigated cation retention using bench-scale positively charged LbL NF membranes with synthetic water. Their study indicated that Mg^{2+} exhibited greater retention than Ca^{2+}, followed by Na^+, owing to differences in hydrated radius and ionic radius (Table 8). Consistent with Cheng et al. [9], experiments conducted on the pilot-scale with WPJ pre-treated IJsselmeer water yielded similar findings, with the retention order of $Mg^{2+} > Ca^{2+} > Na^+$ (Fig. 4). Conversely, experiments with raw IJsselmeer water on the pilot-scale revealed a retention order of $Ca^{2+} > Mg^{2+} > Na^+$ (Fig. 5). The slightly elevated rejection of Ca^{2+} compared to Mg^{2+} (25% over 21% at 70% recovery with raw IJsselmeer water) could potentially be linked to higher NOM concentrations in raw IJsselmeer water compared to WPJ pre-treated IJsselmeer water (Table 2). Divalent ions like Ca^{2+} have a

tendency to form complexes with NOM by binding to the acidic functional groups of NOM (such as the carboxylic group) in surface water, thereby increasing the size of the molecule.

The ions Cl^- and NO_3^- exhibited negative retention (Figs. 4 and 5). Negative retention of ions in NF can be elucidated by the principle of charge neutrality [25]. LbL hollow fiber NF membranes are primarily designed to reject divalent ions over monovalent ions. The monovalent ions Cl^- and NO_3^- compete with the divalent ion SO_4^{2-} and the monovalent ion HCO_3^- (which have a larger hydrated radius than Cl^- and NO_3^-, as shown in Table 8). The membrane's permeability to SO_4^{2-} and HCO_3^- is lower than its permeability to Cl^- and NO_3^-. In order to maintain charge neutrality on both sides of the membrane, the only anions available to neutralize the permeate stream are Cl^- and NO_3^- [26,27]. Consequently, Cl^- and NO_3^- are transported to the permeate side, resulting in the negative retention of these two ions.

The influence of recovery, flux, and crossflow velocity on the ion retention was assessed by varying process conditions throughout each experimental round. Recovery was incrementally increased from 70% to 80% and to 90% in rounds A, B, and C with WPJ pre-treated IJsselmeer water and rounds F, G, and H with raw IJsselmeer water (refer to Table 4). An increase in recovery from 70% to 90% resulted in a notable reduction in ion retention for both WPJ pre-treated IJsselmeer water (Fig. 4) and raw IJsselmeer water (Fig. 5). Generally, higher recovery values result in elevated ion concentrations in the crossflow loop, consequently yielding higher permeate concentrations (assuming consistent membrane retention), and thereby lower ion retentions. This observation was confirmed by an increased concentration factor from 1.58 at 70% recovery to 2.06 at 90% recovery for Ca^{2+}. A decline in ion

retention was also documented by Song et al. [14] in their study involving pilot-scale spiral wound NF membranes, where recovery values increased from 40% to 65%, accompanies by a corresponding rise in concentration factor values from 1.25 to 1.52. Nevertheless, the reduction in retention for SO_4^{2-} was less pronounced (1% decrease) compared to the decrease observed for SO_4^{2-} in raw IJsselmeer water (44% decrease), which may be attributed to the different selective layer chemistry employed in a spiral wound NF thin film composite membrane.

Flux was increased from 20 LMH to 25 LMH in rounds C and D with WPJ pre-treated IJsselmeer water and rounds F and I with raw IJsselmeer water (Table 4). This increase in flux exhibited minimal impact on ion retention with WPJ pre-treated IJsselmeer water (Fig. 4), whereas a reduction in ion retention was observed with the increased flux using raw IJsselmeer water (Fig. 5). The decrease in ion retention with elevated flux on raw IJsselmeer water could potentially be attributed to the increase in permeability from 8.5 LMH/bar in round F to 9.8 LMH/bar in round I (Fig. 3a). An increase in permeability implies a larger pore size in the membrane, thereby facilitating increased ion passage [7]. Round C exhibited an identical permeability value as round D, namely 7.2 LMH/bar (Fig. 2a), confirming the minimal impact on ion retention with pre-treated IJsselmeer water. Additionally, an increase in flux can lead to heightened diffusive transport of ions to the permeate side. With increasing flux, concentration polarization near the membrane intensifies, resulting in a decline in ion retention [20,28]. An increased flux may also enhance convective transport across the membrane, leading to greater feed water passing to the permeate side [28]. Consequently, the ion concentration gets diluted in a larger volume of water on the permeate side, resulting in higher ion retention. It appears that with raw IJsselmeer water, ion retention may be more influenced by diffusive transport than convective transport due to the decrease in ion retention with elevated flux. This could potentially be linked to the low crossflow velocity (0.2 m/s), which amplifies the effect of concentration polarization near the membrane.

Crossflow velocity was increased from 0.2 m/s in round C to 0.3 m/s in round E with WPJ pre-treated IJsselmeer water, and from 0.2 m/s in round F to 0.5 m/s in round J with raw IJsselmeer water (Table 4). Interestingly, an increase in crossflow velocity corresponded with a reduction in ion retention, observed in both pre-treated IJsselmeer water (Fig. 4) and raw IJsselmeer water (Fig. 5). This finding contradicts existing literature. Typically, an increase in crossflow velocity would result in a decrease in concentration polarization and therefore a reduction in the thickness of the boundary layer near the membrane surface. This would subsequently lead to a decrease in diffusive transport across the membrane [29,30], consequently increasing ion retention. Junker et al. [4] observed an increase in MgSO₄ retention with elevated crossflow velocity using both bench-scale and pilot-scale LbL hollow fiber NF membranes with synthetic water. The decrease in ion retention with increased crossflow velocity on the dNF40 membrane could possibly be attributed to the increase in permeability between round C (7.2 LMH/bar) and round E (8.2 LMH/bar) for pre-treated IJsselmeer water (Fig. 2a), and round F (8.5 LMH/bar) and round J (10.3 LMH/bar) for raw IJsselmeer water (Fig. 3a). An increase in permeability with elevated crossflow velocity could potentially be attributed to temperature elevation or other operational parameters. An increase in temperature potentially signifies a larger apparent pore size in the membrane, facilitating greater ion passage [7]. Further investigation into this phenomenon will be conducted in Chapter 3.3.

In summary, the experiments revealed intriguig trends. Increasing recovery led to a notable reduction in ion retention, particularly for Ca^{2+} ions, across both WPJ pre-treated and raw IJsselmeer water. Flux had minimal impact on ion retention with pre-treated IJsselmeer water but resulted in decreased retention for raw IJsselmeer water, likely due to increased permeability. Surprisingly, higher crossflow velocity corresponded with reduced ion retention for both water types, contrary to literature findings. This unexpected trend suggests a need for further investigation into the underlying factors, such as increased permeability due to temperature elevation, to better understand ion retention mechanisms under varying operational conditions.

3.3. Comparison between pre-treated and raw IJsselmeer water

From Figs. 2a and 3a, it is evident that the permeability remained stable under constant process conditions within each interval. Fig. 6 illustrates the average permeability, temperature-corrected, for rounds A, B and C with WPJ pre-treated IJsselmeer water, and rounds F, G and H with raw IJsselmeer water. Filtration rounds utilizing WPJ pre-treated IJsselmeer water were conducted employing the pristine dNF40 module, while the subsequent experiments with raw IJsselmeer water were performed utilizing the same dNF40 module one year later. Additionally, Fig. 7 depicts the ion retention with increasing recovery from 70% to 90% for rounds A, B and C with WPJ pre-treated IJsselmeer water and rounds F, G and H with raw IJsselmeer water. Notably, filtration rounds with raw IJsselmeer water exhibited diminished retention values compared to those with WPJ pre-treated IJsselmeer water, particularly concerning the divalent ions SO_4^{2-}, Ca^{2+}, and Mg^{2+}.

An increase in permeability of 1.5 LMH/bar was observed during operation with raw IJsselmeer water in comparison to WPJ pre-treated IJsselmeer water, utilizing the same membrane and under similar feed water temperature conditions (Fig. 6). Consequently, a reduction in ion retention was observed during filtration with raw IJsselmeer water relative to WPJ pre-treated IJsselmeer water (Fig. 7). The lower ion retention during filtration with raw IJsselmeer water was accompanied by an increase in permeability. A higher permeability can imply larger pore sizes in the membrane or a thinner active membrane layer [7], facilitating increased ion passage through the membrane. The observed increase in permeability by 1.5 LMH/bar over long-term operation contrasts with findings in the literature. In a long-term study, Beyer et al. [15] reported a decrease in permeability of NF membranes after 5 years of operation, while Jafari et al. [17] noted similar trends in RO membranes after 2 years of operation, predominantly attributed to fouling formation. Even chemical cleaning procedures proved inadequate in restoring the permeability of these membranes to their original levels. Furthermore, RO membranes are recognized to experience an increase in solute passage over time, as indicated by an increase in salt permeability coefficient [31,32].

An integrity test was executed utilizing a direct cell count (DCC) to evaluate the presence of potential broken fibers within the membrane element. NF membranes are recognized for their capacity to eliminate bacteria and viruses by at least 4 logs, whereas fiber failure typically diminishes removal efficacy to less than 2 logs [33]. The log-removal of the dNF40 membrane was evaluated through DCC analysis. As shown in Table 9, both DCC-living and DCC-total log-removal values are approximately 4 logs, indicative of the typical log-removal for NF membranes. This indicates that fiber failure is unlikely to be the cause of the observed higher permeability and lower ion retention. Additionally, a pressure decay test conducted on the membrane module confirmed the absence of broken fibers within the membrane.

The surprising observed increase in permeability over the long term may be attributed to the change in membrane active layer properties caused by multiple CIP events (due to insufficient flushing process after every CIP cycle), as depicted in Fig. 3a. Moreover, temperature can also play a role in an observed permeability trend as explained before in Chapter 3.1 and 3.2. A possible explanation for the permeability increase could be the excessive frequency of chemical cleaning; the dNF40 membrane underwent 21 CIP cycles within its last operational year, surpassing the recommended limit of 13 CIP cycles per year at full scale [34]. Another potential factor contributing to the increased permeability might be the insufficient flushing duration of the module between high pH and low pH cleaning, resulting in the production of chemical species that could impact the membrane. Inadequate removal of NaOCl and NaOH residues may lead to the formation of free residual chlorine
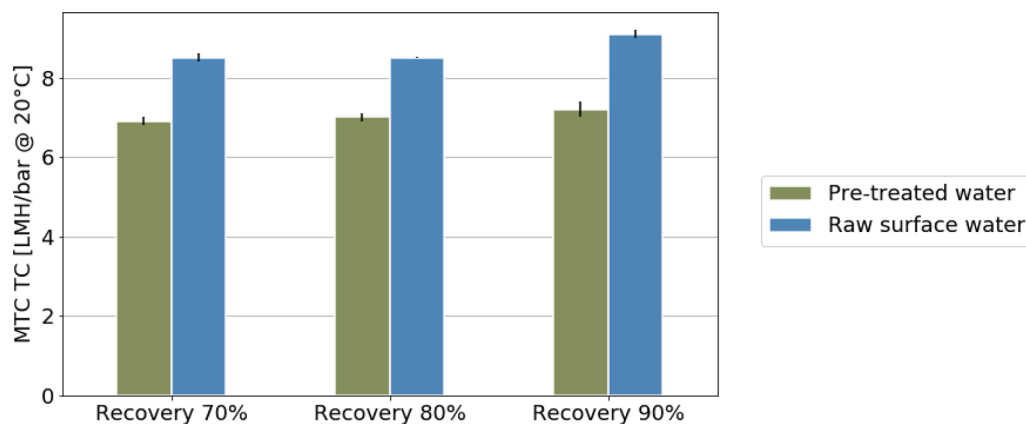
Fig. 6. Average temperature corrected permeability of WPJ pre-treated IJsselmeer water (green bars) and raw IJsselmeer water (blue bars) at 70%, 80%, and 90% recovery, 20 LMH flux, and 0.2 m/s crossflow velocity. (For interpretation of the references to colour in this figure legend, the reader is referred to the web version of this article).
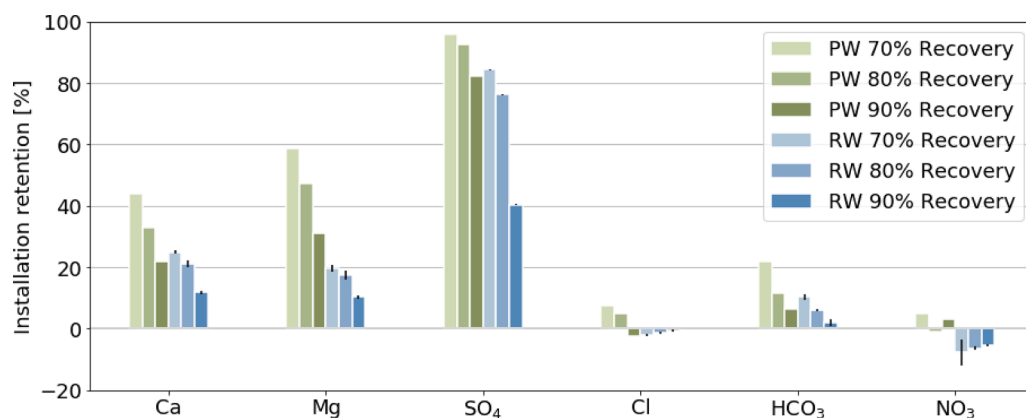

Fig. 7. Ion installation retention based on concentrations measured in feed stream and permeate stream during filtration with pre-treated IJsselmeer water (green bars) and raw IJsselmeer water (blue bars) at 70%, 80%, and 90% recovery, 20 LMH flux, and 0.2 m/s crossflow velocity. PW stands for WPJ pre-treated IJsselmeer water and RW stands for raw IJsselmeer water. (For interpretation of the references to colour in this figure legend, the reader is referred to the web version of this article).

Table 9
The concentration of DCC-living and DCC-total in the feed and permeate stream and the log-removal.

	Feed concentration [cells/ml]	Permeate concentration [cells/ml]	Log-removal
DCC-living	830,000	40	4.3
DCC-total	1,764,000	215	3.9

upon reaction with citric acid [35], which could adversely affect the membrane support [36]. Moreover, exposure of an RO membrane to free residual chlorine can induce irreversible changes in the structure of the active layer, causing an increase in water flux and a reduction in salt retention [37]. Nevertheless, further comprehensive research is needed to ascertain whether the membrane properties were affected by the excessive frequency of chemical cleaning or insufficient flushing duration.

3.4. NOM removal

The efficacy of NOM removal using the dNF40 membrane was examined in Table 10 through experiments conducted under varied process conditions (Table 4) using both WPJ pre-treated and raw

Table 10
Feed concentration TOC and TOC removal based on concentrations measured in feed and permeate stream during filtration with pre-treated and raw IJsselmeer water.

	Water type	Feed concentration [mg/L C]	TOC removal [%]
Round A	Pre-treated IJsselmeer	3.5	97
Round B		3.6	96
Round C		3.6	92
Round D		3.7	96
Round E		3.1	87
Round F	Raw IJsselmeer	5.8 ± 0.31	95 ± 0.01
Round G		6.1 ± 0.31	95 ± 0.65
Round H		6.3 ± 0.15	92 ± 0.13
Round I		6.5 ± 0.29	95 ± 0.26
Round J		6.2 ± 0.16	93 ± 0.26

IJsselmeer water. The quantification of NOM in water primarily relies on measuring the total organic carbon (TOC). TOC removal was determined by comparing concentrations measured in the feed and permeate. Table 10 presents the feed concentration and TOC removal achieved by the dNF40 membrane during each filtration round. The average TOC

concentration in WPJ pre-treated IJsselmeer water was 3.5 mg/L C, whereas in raw IJsselmeer water, it averaged 6.2 mg/L C.

The TOC removal consistently exceeded 87% across all water types and process conditions. These consistently high removal percentages indicate that variations in process conditions, such as recovery, flux, or crossflow velocity did not significantly affect TOC removal. This robust removal performance can be attributed to the fact that the pore size of the dNF40 membrane is generally smaller than that of typical organic compounds. Similar high TOC removal percentages have been reported in the literature. For instance, Haddad et al. [38] demonstrated that NOM removal using a bench-scale crossflow filtration setup equipped with thin-film hollow fiber NF membranes with a molecular weight cutoff (MWCO) of 200 Da, operated with synthetic water, consistently exceeded 90%.

An LC-OCD analysis was conducted on round F to depict the fraction of TOC removed by the membrane. TOC encompasses various fractions, including acids, biopolymers (BP), building blocks (BB), hydrophobic organic compounds (HOC), humic substances (HS), neutrals, and particulate organic matter (POC). Fig. 8 illustrates the NOM removal of TOC fractions during filtration round F (using raw IJsselmeer water, 70% recovery, 20 LMH flux, and 0.2 m/s crossflow velocity). It is noteworthy that the removal of the acids and POC fractions was not analysed due to their low concentrations in the feed stream (0 µg/L C and 10.5 µg/L C, respectively).

Typically, NOM exhibits high molecular weights and a negative charge, particularly within the pH range of natural waters. Consequently, the removal mechanisms employed by hollow fiber NF membranes to eliminate NOM fractions involve both size (steric) exclusion and Donnan (charge) exclusion [38]. The characteristics of the various fractions are outlined in Table 11.

The BP and HS fractions, with molecular weight values exceeding the MWCO of the dNF40 membrane (400 Da), exhibited the highest removal percentages: 99.4% and 97.8%, respectively. Conversely, BB fractions and neutrals possess molecular weight values around or below the MWCO of the dNF40 membrane. However, BB fractions, being negatively charged, demonstrated a higher removal percentage compared to neutrals, namely 96.1% for BB fractions and 88.7% for neutrals. This trend aligns with the substantial retention observed for negatively charged ions like SO_4^{2-}. Similar observations were reported by Meylan et al. [39] and Owusu-Agyeman et al. [40], who found higher removal percentages for BP, HS, and BB fractions compared to neutrals using NF membranes. Furthermore, Meylan et al. [39] demonstrated that bench-scale negatively charged NF membranes generally retain neutrals less effectively than negatively charged compounds with comparable molecular weights (e.g., acids or BB fractions). The HOC fraction exhibited the lowest removal percentage at 46.1% (Fig. 8). In LC-OCD analysis,
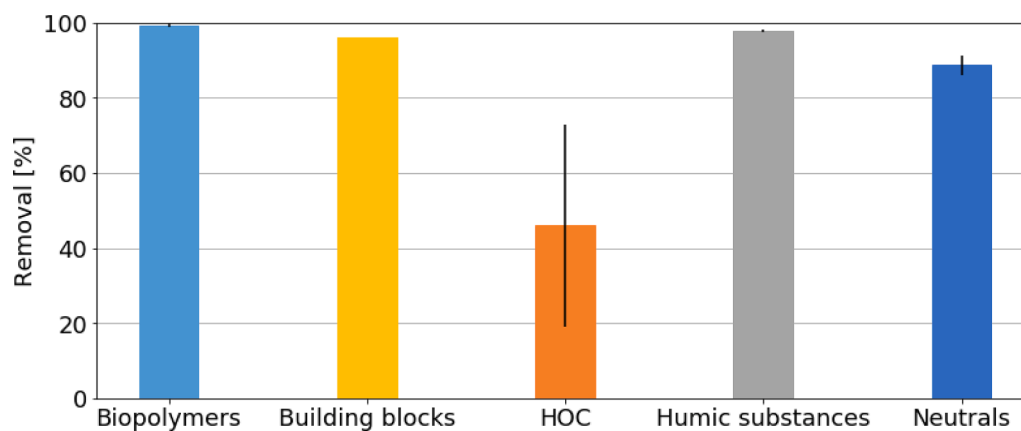
Table 11
Properties of the fractions of NOM [38].

Fraction	Hydrophobic or hydrophilic	Charge	MW [g/mol]
Acids	N.A.	–	<350
Biopolymers	Hydrophilic	0	>10.000
Building blocks	Hydrophilic	–	300–500
HOC	Hydrophobic	0	N.A.
Humic substances	Hydrophilic	–	800–1000
Neutrals	Hydrophilic	0	<350

HOC is calculated as the difference between DOC and the sum of BP, HH, BB, acids, and neutrals. Due to its hydrophobic nature, the HOC fraction tends to adsorb onto the column, resulting in inaccurate measurements via LC-OCD analysis [41]. This could introduce uncertainties in the removal percentage of HOC by the dNF40 membrane, as evidenced by the high standard deviation between individual samples.

3.5. PFAS retention

The retention of PFAS with the dNF40 membrane was assessed in Fig. 9 through experiments conducted using spiked WPJ pre-treated IJsselmeer water at 70% recovery, 30 LMH flux, and 0.2 m/s crossflow velocity. The intended concentrations of PFAS in the spiked solution are outlined in Table 5. In Fig. 9, the purple bars represent PFAS retention based on the background PFAS in WPJ pre-treated IJsselmeer water, while the yellow bars depict PFAS retention based on the spiked solution added to WPJ pre-treated IJsselmeer water. The background PFAS compounds exhibited retention values ranging from 71% to 100%, whereas the spiked PFAS compounds demonstrated retention values ranging from 86% to 93%.

When interpreting the results, a clear distinction is made between the four background PFAS bars and the four spiked PFAS bars. Size (steric) exclusion emerges as the primary retention mechanism over Donnan (charge) exclusion, particularly for high molecular weight PFAS compounds [10,42]. Both background PFAS and spiked PFAS exhibited an increase in retention values with rising molecular weight due to size (steric) exclusion (Fig. 9), with the exception of PFNA, which showed a slight decrease in retention value compared to PFOA. Similarly, an increase in retention values with higher molecular weight was noted by Liu et al. [43] using pilot-scale, spiral wound NF membranes, and by Appleman et al. [44] using bench-scale, flat-sheet NF membranes. However, the retention values for low molecular weight PFBA and PFBS were relatively lower (<70%) compared to the aforementioned studies, where retention values consistently exceeded 90% for all PFAS. This variance can be attributed to the higher MWCO of the dNF40 membrane (400 Da) compared to 180 Da for the membrane in Liu et al. [43] and

Fig. 8. Fractions of NOM removal based on concentrations measured in feed stream and permeate stream during filtration with raw Ijsselmeer water at 70 % recovery, 20 LMH flux, and 0.2 m/s crossflow velocity. (For interpretation of the references to colour in this figure legend, the reader is referred to the web version of this article).
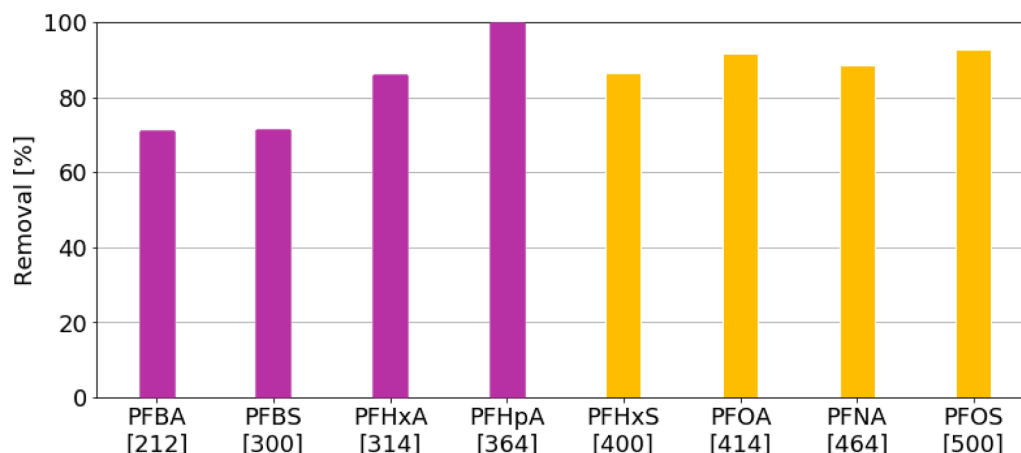
Fig. 9. PFAS retention based on concentrations measured in feed stream and permeate stream during filtration with spiked WPJ pre-treated IJsselmeer water. The purple bars show PFAS retention based on background PFAS concentrations in pre-treated IJsselmeer water. The yellow bars show PFAS retention based on spiked concentrations in pre-treated IJsselmeer water. The number in between the brackets is the molecular weight of the PFAS compound. The PFAS compounds are sorted based on molecular weight. (For interpretation of the references to colour in this figure legend, the reader is referred to the web version of this article).

between 150——200 Da for the membrane in Appleman et al. [44].

The concentrations of background PFAS (including PFBA and PFBS) measured in the permeate were below the detection limit; therefore, these bars only indicate the minimum retention of these PFAS compounds. Conversely, the spiked PFAS compounds demonstrated retention values above 80%, consistent with findings in the literature. Wang et al. [10] demonstrated retention values above 80% for high molecular weight PFAS compounds PFOA and PFOS using bench-scale negative LbL hollow fiber NF membranes.

3.6. Pharmaceutical retention

The retention of pharmaceuticals using the dNF40 membrane was assessed in Fig. 10 through experiments conducted with spiked WPJ pre-treated IJsselmeer water under conditions of 70% recovery, 30 LMH flux, and 0.2 m/s crossflow velocity. The target concentrations of pharmaceuticals in the spiked solution are detailed in Table 5.

The retention of uncharged pharmaceuticals primarily occurs through size (steric) exclusion, whereas for charged pharmaceuticals, it involves a combination of size (steric) exclusion and Donnan (charge) exclusion. Table 12 provides an overview of the chemical and physical properties of the spiked pharmaceuticals. All pharmaceuticals tested have molecular weights below the MWCO of the dNF40 membrane, which is 400 Da. Therefore, establishing a direct relationship between molecular weight and retention for a specific pharmaceutical is challenging. Notably, the compound pyrazol exhibited negative retention by the membrane (Fig. 10). Given its neutral charge, pyrazol is retained solely via size (steric) exclusion, with its small molecular weight contributing to its limited retention by the dNF40 membrane.

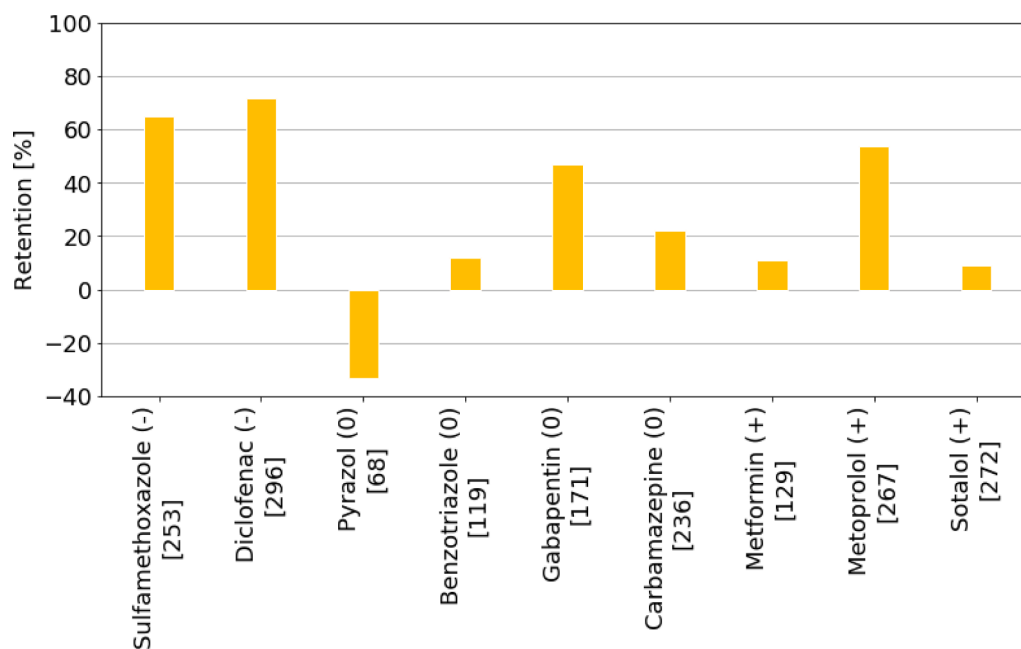The membrane exhibited better retention of negative

Fig. 10. Pharmaceutical retention based on concentrations measured in feed stream and permeate stream during filtration with spiked pre-treated IJsselmeer water. The symbol between the parentheses represent the charge of the pharmaceutical, in which − is negative, 0 is neutral and + is positive. The number between the square brackets is the molecular weight of the pharmaceutical. The pharmaceuticals are sorted based on charge and within the charged groups based on molecular weight.

Table 12

Chemical and physical properties of pharmaceuticals in the spiked solution. The values were taken from Ebrahimzadeh et al. [44].

Name	MW [g/mol]	Charge
Pyrazol	68	0
Benzotriazole	119	0
Metformin	129	+
Gabapentin	171	0
Carbamazepine	236	0
Sulfamethoxazole	253	−
Metoprolol	267	+
Sotalol	273	+
Diclofenac	296	−

pharmaceuticals compared to neutral and positive ones. This phenomenon can be attributed to the negative terminal layer of the dNF40 membrane, which demonstrated typical Donnan (charge) exclusion behavior, resulting in higher retention values for negative pharmaceuticals. This is similar to the higher retention observed for SO_4^{2-}. Similar findings were reported by De Grooth et al. [8] using bench-scale hollow fiber NF membranes with a negative charge terminal layer, further supporting the notion of enhanced retention of negative pharmaceuticals. Dagher et. al. [45] similarly investigated the retention behavior of negatively charged and neutral pharmaceuticals using bench-scale hollow fiber NF membranes with a negative charge terminal layer. Their research revealed that the membrane exhibited increased retention of negatively charged pharmaceuticals, with retention values consistently exceeding 80%. Additionally, in the research conducted by Dagher et.al. [45], Neutral pharmaceuticals with molecular weights above 200 Da demonstrated retention values exceeding 80%. Notably, similar to this study, neutral compounds with molecular weights below 200 Da exhibited retention values ranging between 4% and 80%.

3.7. Economic feasibility

A full-scale treatment plant incorporating 5 stages of dNF40 membranes was designed utilizing the specifications outlined in Table 6 and the raw IJsselmeer feed water quality (Table 2). Operational and capital expenditures (OPEX and CAPEX) were projected for producing 15 million cubic meters of permeate annually at a recovery rate of 85%. Each stage within the 5-stage system achieves a membrane recovery of 17.3%, cumulatively contributing to the system's overall recovery of 85%. The quality of permeate water is optimal in the initial stage and progressively deteriorates in subsequent stages. The concentration polarization factors intensifies as the ion concentration in the concentrate increases with each stage. The dNF40 pilot setup mimics the final stage within a full-scale dNF40 plant.

OPEX was determined by considering energy costs, chemical costs, and membrane replacement costs, whereas CAPEX was derived from equipment and installation costs [11]. Both OPEX and CAPEX were computed in terms of €/m³ of permeate water. Specifically, the OPEX for the 5-stage full-scale dNF40 plant amounted to 0.08 €$_{OPEX}$/m³ of permeate water, while the CAPEX for the same plant configuration was 0.03 €$_{CAPEX}$/m³ of permeate water.

The OPEX per m³ of permeate water was a factor three times higher than the CAPEX per m³ of permeate water. This discrepancy is due to the continuous nature of OPEX requirements, in contrast to the one-time occurrence of CAPEX at the commencement of a 20-year operational period [11]. Although the CAPEX estimation excluded costs associated with land acquisition, planning, and construction of buildings due to the highly specific and variable nature of these factors, their inclusion would likely elevate CAPEX, although still not surpassing OPEX [11]. A comparison of the OPEX and CAPEX with literature values for UF-RO costs reveals that the OPEX for the dNF40 plant is more economically feasible than that for UF and RO, while CAPEX shows comparable values. For instance, Kehrein et al. [11] reported OPEX and CAPEX values of 0.33

€$_{OPEX}$/m³ of permeate water and 0.03 €$_{CAPEX}$/m³ of permeate water for RO, and 0.11 €$_{OPEX}$/m³ of permeate water and 0.03 €$_{CAPEX}$/m³ of permeate water for UF. The higher OPEX for RO systems may be attributed to the reduced membrane pore size, necessitating increased chemical cleaning and energy expenditures.

Table 13 illustrates the breakdown of energy, chemical, and membrane replacement costs as a percentage of the total OPEX for the full-scale dNF40 plant. The primary cost component within the OPEX was the membrane replacement cost, followed by energy cost, and chemical cost.

4. Conclusion

Through a comprehensive one-year operational study, this pilot scale dNF40 membrane system demonstrated robust performance across various testing conditions, encompassing two distinct water matrices: WPJ pre-treated IJsselmeer water and raw IJsselmeer water. The evaluation of membrane performance parameters such as permeability, transmembrane pressure (TMP) and normalized pressure drop (NPD) revealed stability throughout the testing periods, indicative limited to no fouling impact during operation. Notably, slight variations in permeability, TMP and NPD were observed within each operational condition interval, largely attributed to corresponding temperature fluctuations.

The findings highlight intriguing trends in membrane behavior. Notably, an interesting discrepancy in permeability was observed between pre-treated and raw IJsselmeer water, with the former exhibiting higher permeability, potentially attributable to thorough cleaning-in-place (CIP) procedures. Moreover, alterations in process conditions – namely recovery, flux and crossflow velocity – were as expected found to influence ion retention, with recovery employing the most significant impact on ion compound retention across both water types.

Despite variations in process conditions, the study consistently demonstrated robust removal of natural organic matter (NOM), with removal rates consistently exceeding 90% across all experimental rounds. Similarly, the retention of per- and polyfluoroalkyl substances (PFAS) exceeded 80%, exhibiting an increase with higher molecular weight. However, the retention of pharmaceuticals in the spiked solution was modest, around 30%, primarily attributed to their low molecular weight compared to the membrane's molecular weight cutoff (MWCO). Notably, negatively charged pharmaceuticals exhibited superior retention compared to neutral and positively charged counterparts.

The economic analysis underscores the viability of the dNF40 membrane technology, with operational expenditure (OPEX) being threefold higher than capital expenditure (CAPEX). This discrepancy can be attributed to the continuous nature of OPEX, with membrane replacement emerging as the primary cost driver, followed by energy and chemical costs. Importantly, the study suggest that NF technology offers cost-effective solutions compared to ultrafiltration (UF) and reverse osmosis (RO), particularly in terms of OPEX.

Overall, optimizing CIP protocols to mitigate permeability discrepancies between pre-treated and raw IJsselmeer water matrices, refining operational parameters to enhance ion retention and exploring advanced membrane materials for improved pharmaceutical removal are topics worthy of further investigation. Additionally, the study offers valuable insights into the potential application of dNF40 membrane

Table 13

OPEX factor distribution as a percentage of the total OPEX based on OPEX per m³ permeate water.

	Full-scale dNF40 plant
Energy	31.5 %
Chemical	0.9 %
Membrane	67.6 %

technology, particularly in high fouling potential water applications, either as a direct purification step or as pre-treatment in combination with additional adsorption methods like activated carbon. These recommendations pave the way for informed implementation and optimization of dNF40 membrane systems in water treatment applications.

In light of these findings, the study offers valuable insights and recommendations for future applications of dNF40 membrane technology. The technology demonstrated robust performance, particularly suited for high fouling potential water applications. Its exceptional performance in fouling control, coupled with its acceptable retention of PFAS, positions hollow fiber nanofiltration technology as a promising candidate for direct purification or even standalone application. Additionally, it could be effectively employed as pre-treatment in combination with additional adsorption methods such as activated carbon.

CRediT authorship contribution statement

Marleen Ophorst: Writing – original draft, Visualization, Validation, Resources, Methodology, Investigation, Formal analysis, Data curation, Conceptualization. **Joris de Grooth:** Writing – review & editing, Resources, Conceptualization. **Sebastiaan G.J. Heijman:** Writing – review & editing, Supervision. **Elisabeth M.H. Vaudevire:** Writing – review & editing, Formal analysis. **Morez Jafari:** Writing – review & editing, Validation, Supervision, Formal analysis, Data curation, Conceptualization.

Declaration of competing interest

The authors declare that they have no known competing financial interests or personal relationships that could have appeared to influence the work reported in this paper.

Data availability

Data will be made available on request.

References

[1] Y. Luo, W. Guo, H.H. Ngo, L.D. Nghiem, F.I. Hai, J. Zhang, S. Liang, X.C. Wang, A review on the occurrence of micropollutants in the aquatic environment and their fate and removal during wastewater treatment, Sci. Total Environ. 473–474 (2014) 619–641.

[2] S.P. Lenka, M. Kah, L.P. Padhye, A review of the occurrence, transformation, and removal of poly- and perfluoroalkyl substances (PFAS) in wastewater treatment plants, Water Res. 199 (2021).

[3] J.L. Domingo, M. Nadal, Human exposure to per- and polyfluoroalkyl substances (PFAS) through drinking water: A review of the recent scientific literature, Environ. Res. 177 (2019).

[4] M.A. Junker, W.M. de Vos, R.G.H. Lammertink, J. de Grooth, Bridging the gap between lab-scale and commercial dimensions of hollow fiber nanofiltration membranes, J. Membr. Sci. 624 (2021).

[5] T. Sewerin, M.G. Elshof, S. Matencio, M. Boerrigter, J. Yu, J. de Grooth, Advances and applications of hollow fiber nanofiltration membranes: a review, Membranes 11 (11) (2021) pp.

[6] M. Frank, G. Bargeman, A. Zwijnenburg, M. Wessling, Capillary hollow fiber nanofiltration membranes, Sep. Purif. Technol. 22–23 (2001) 499–506.

[7] N. Joseph, P. Ahmadiannamini, R. Hoogenboom, I.F.J. Vankelecom, Layer-by-layer preparation of polyelectrolyte multilayer membranes for separation, Polym. Chem. 5 (2014) 1817–1831.

[8] J. de Grooth, D.M. Reurink, J. Ploegmakers, W.M. de Vos, K. Nijmeijer, Charged micropollutant removal with hollow fiber nanofiltration membranes based on polycation/polyzwitterion/polyanion multilayers, ACS Appl. Mater. Interfaces 6 (19) (2014) pp.

[9] W. Cheng, C. Liu, T. Tong, R. Epsztein, M. Sun, R. Verduzco, J. Ma, M. Elimelech, Selective removal of divalent cations by polyelectrolyte multilayer nanofiltration membrane: Role of polyelectrolyte charge, ion size, and ionic strength, J. Membr. Sci. 559 (2018) 98–106.

[10] Y. Wang, I. Zucker, C. Boo, M. Elimelech, Removal of emerging wastewater organic contaminants by polyelectrolyte multilayer nanofiltration membranes with tailored selectivity, ACS ES&T Eng. 1 (3) (2021) 404–414.

[11] P. Kehrein, M. Jafari, M. Slagt, E. Cornelissen, P. Osseweijer, J. Posada, M. Van Loosdrecht, A techno-economic analysis of membrane-based advanced treatment processes for the reuse of municipal wastewater, Water Reuse 11 (4) (2021) 705–725.

[12] M. Jafari, M. Vanoppen, J.M.C. Van Agtmaal, E.R. Cornelisen, J.S. Vrouwenvelder, A. Verliefde, M.C.M. Van Loosdrecht, C. Picioreanu, Cost of fouling in full-scale RO & NF installations in The Netherlands, Desalination 500 (2021).

[13] J.E. Kilduff, S. Mattaraj, G. Belfort, Flux decline during nanofiltration of naturally occuring dissolved organic matter: effects of osmotic pressure, membrane permeability and cake formation, J. Membr. Sci. 239 (1) (2004) 39–53.

[14] Y. Song, X. Gao, T. Li, C. Gao, J. Zhou, Improvement of overall water recovery by increasing RNF with recirculation in a NF-RO integrated membrane process for seawater desalination, Desalination 364 (2015) 95–104.

[15] F. Beyer, B.M. Rietman, A. Zwijnenburg, P.v.d Brink, J.S. Vrouwenvelder, M. Jarzembowska, J. Laurinonyte, A.J.M Stams, C.M. Plugge, Long-term performance and fouling analysis of full-scale direct nanofiltration (NF) installations treating anoxic groundwater, J. Membr. Sci. 468 (2014) 339–348.

[16] F. Beyer, J. Laurinonyte, A. Zwijnenburg, A.J.M. Stams, C.M. Plugge, Membrane fouling and chemical cleaning in three full-scale reverse osmosis plants producing demineralized water, J. Eng. 2017 (2017).

[17] M. Jafari A. D`haese J. Zlopasa E.R. Cornelissen J.S. Vrouwenvelder K. Verbeken A. Verliefde M.C.M. van Loosdrecht C. Picioreanu A comparison between chemical cleaning efficiency in lab-scale and full-scale reverse osmosis membranes: Role of extracellular polymeric substances (EPS) Journal of Membrane Science 609 2020.

[18] C. Ba, D.A. Ladner, J. Economy, Using polyelectrolyte coatings to improve fouling resistance of a positively charged nanofiltration membrane, J. Membr. Sci. 347 (1–2) (2010) 250–259.

[19] A.W. Zularisam, A.F. Ismail, R. Salim, Behaviours of natural organic matter in membrane filtration for surface water treatment - a review, Desalination 194 (1–3) (2006) 211–231.

[20] M.M. Emamjomeh, H. Torabi, M. Mousazadeh, M.H. Alijani, F. Gohari, Impact of independent and non-independent parameters on various elements' rejection by nanofiltration employed in groundwater treatment, Appl. Water Sci. 9 (71) (2019) pp.

[21] Z. He, D.J. Miller, S. Kasemset, D.R. Paul, B.D. Freeman, The effect of permeate flux on membrane fouling during microfiltration of oily water, J. Membr. Sci. 525 (2017) 25–34.

[22] H. Choi, K. Zhang, D.D. Dionysiou, D.B. Oerther, G.A. Sorial, Influence of cross-flow velocity on membrane performance during filtration of biological suspension, J. Membr. Sci. 248 (1–2) (2005) 189–199.

[23] E. Virga, K. Žvab, W. de Vos, Fouling of nanofiltration membranes based on polyelectrolyte multilayers: the effect of a zwitterionic final layer, J. Membr. Sci. 620 (2021).

[24] D.M. Reurink, E. Te Brinke, I. Achterhuis, H.D.W. Roesink, W.M. de Vos, Nafion-based low-hydration polyelectrolyte multilayer membranes for enhanced water purification, ACS Appl. Polym. Mater. 1 (9) (2019) 2543–2551.

[25] A.E. Yaroshchuk, Negative rejection of ions in pressure-driven membrane processes, Adv. Colloid Interface Sci. 139 (1–2) (2008) 150–173.

[26] O. Labban, C. Liu, T.H. Chong, J.H. Lienhard, Fundamentals of low-pressure nanofiltration: Membrane characterization, modeling, and understanding the multi-ionic interactions in water softening, J. Membr. Sci. 521 (2017) 18–32.

[27] M. Reig, N. Pagès, E. Licon, C. Valderrama, O. Gibert, A. Yaroshchuk, J.L. Cortina, Evolution of electrolyte mixtures rejection behaviour using nanofiltration membranes under spiral wound and flat-sheet configurations, Desalin. Water Treat. 56 (13) (2015) 3519–3529.

[28] B.A.M. Al-Rashdi, D.J. Johnson, N. Hilal, Removal of heavy metal ions by nanofiltration, Desalination 315 (2013) 2–17.

[29] J. Fernández-Sempere, F. Ruiz-Beviá, P. García-Algado, R. Salcedo-Díaz, Experimental study of concentration polarization in a crossflow reverse osmosis system using Digital Holographic Interferometry, Desalination 257 (1–3) (2010) 36–45.

[30] R. Bian, K. Yamamoto, Y. Watanabe, The effect of shear rate on controlling the concentration polarization and membrane fouling, Desalination 131 (1–3) (2000) 225–236.

[31] N. Al-Bastaki, A. Abbas, Long-term performance of an industrial water desalination plant, Chem. Eng. Process. 43 (4) (2004) 555–558.

[32] M. Wilf, K. Klinko, Performance of commercial seawater membranes, Desalination 96 (1–3) (1994) 465–478.

[33] A. Lidén, E. Lavonen, K.M. Persson, M. Larson, Integrity breaches in a hollow fiber nanofilter – Effects on natural organic matter and virus-like particle removal, Water Res. 105 (2016) 231–240.

[34] NXFiltration, "WRC200 dNF40 Integrated Rack Design Hollow fiber nanofiltration membrane module for water and wastewater applications". *Technical datasheet.*

[35] P.P. Wright, B. Kahler, L.J. Walsh, "Alkaline sodium hypochlorite irrigant and its chemical interactions," *Materials (Basel, Switzerland),* vol. 10, no. 10, 2017.

[36] C. Causseran, B. Pellegrin, J.C. Rouch, Effects of sodium hypochlorite exposure mode on PES/PVP ultrafiltration membrane degradation, Water Res. 85 (2015) 316–326.

[37] J.M. Gohil, A.K. Suresh, Chlorine attack on reverse osmosis membranes: mechanisms and mitigation strategies, J. Membr. Sci. 541 (2017) 108–126.

[38] M. Haddad, T. Ohkame, P.R. Bérubé, B. Barbeau, Performance of thin-film composite hollow fiber nanofiltration for the removal of dissolved Mn, Fe and NOM from domestic groundwater supplies, Water Res. 145 (2018) 408–417.

[39] S. Meylan, F. Hammes, J. Trabel, E. Salhi, U. von Gunten, W. Pronk, Permeability of low molecular weight organics through nanofiltration membranes, Water Res. 41 (17) (2007) 3968–3976.

[40] I. Owusu-Agyeman, M. Reinwald, A. Jeihanipour, A.I. Schäfer, Removal of fluoride and natural organic matter from natural tropical brakisch waters by nanofiltration/ reverse osmosis with varying water chemistry, Chemosphere 217 (2019) 47–58.

[41] S.A. Huber, A. Balz, M. Abert, W. Pronk, Characterisation of aquatic humic and non-humic matter with size-exclusion chromatography - organic carbon detection - organic nitrogen detection (LC-OCD-OND), Water Res. 45 (2) (2011) 879–885.

[42] J. Xiong, Y. Hou, J. Wang, Z. Liu, Y. Qu, Z. Li, X. Wang, The rejection of perfluoroalkyl substances by nanofiltration and reverse osmosis: Influencing factors and combination processes, Environ. Sci. Water Res. Technol. 7 (2021) 1928–1943.

[43] C.J. Liu, T.J. Strathmann, C. Bellona, Rejection of per- and polyfluoroalkyl substances (PFASs) in aqueous film-forming foam by high-pressure membranes, Water Res. 188 (2020).

[44] T.D. Appleman, E.R.V. Dickenson, C. Bellona, C.P. Higgins, Nanofiltration and granular activated carbon treatment of perfluoroalkyl acids, J. Hazard. Mater. 260 (2013) 740–746.

[45] G. Dagher, G. Saab, A. Martin, G. Couturier, P. Candido, L. Moulin, J.P. J. P. Croué en B. Teychene, Understanding and predicting the adsorption and rejection of pesticides and metabolites by hollow fiber nanofiltration membranes, Separ. Purif. Technol. 330 (2023).